Realistic tight-binding model for the electronic structure of II-VI semiconductors

Sameer Sapra, N. Shanthi, and D. D. Sarma*
Solid State and Structural Chemistry Unit, Indian Institute of Science, Bangalore 560012, India
(Received 27 June 2002; published 18 November 2002)

We analyze the electronic structure of group II-VI semiconductors obtained within linearized muffin-tin-orbital approach in order to arrive at a realistic and minimal tight-binding model, parametrized to provide an accurate description of both valence and conduction bands. It is shown that a nearest-neighbor sp^3d^5 model is fairly sufficient to describe the electronic structure of these systems over a wide energy range, obviating the use of any fictitious s^* orbital. The obtained hopping parameters obey the universal scaling law proposed by Harrison, ensuring transferability to other systems. Furthermore, we show that certain subtle features in the bonding of these compounds require the inclusion of anion-anion interactions in addition to the nearest-neighbor cation-anion interactions.

DOI: 10.1103/PhysRevB.66.205202 PACS number(s): 71.20.Nr

I. INTRODUCTION

The parametrized tight-binding (TB) method has been employed extensively in the past for the study of tetrahedrally coordinated semiconductors due to the simplicity of the approach and its ability to describe properties in terms of chemical bonds. This gives the model a more realistic nature as opposed to methods based on weak periodic potentials.[1–3] The TB approach is suitable to handle larger systems compared to methods based on plane waves, due to the low-computational costs. The TB method was originally described by Slater and Koster as an interpolation scheme.[1] It has been developed extensively since then and is now a well-established technique to elucidate the electronic structure of solids.[3] A tremendous advance in the modern computers along with the development of highly efficient calculational schemes over the past two decades has made it possible to obtain in an *ab initio* manner the electronic structure of almost all compound semiconductors with typically 2–20 atoms in the unit cells, undermining the usefulness of such parametrized tight-binding models. However, over the past one decade, this method is seeing a revival due to the advent of quantum dots and other related nanoscopic sciences. Since semiconductor particles can be routinely prepared today in the nanometric length scale to obtain physical properties that are significantly different from those in the bulk material, there is a need to be able to calculate the electronic structure of such nanoparticles. Since these systems lack the lattice periodicity of the infinite solid, a real-space electronic structure calculation is necessary. Since such systems may contain several thousand atoms, it is impossible to obtain *ab initio* electronic structure information of such systems. Therefore, it becomes absolutely necessary to have simple and yet highly accurate parametrized TB models to describe such systems. Moreover, the availability of a highly accurate parameter set may also allow one to perform molecular dynamical studies of such systems containing much larger number of atoms than can be handled within *ab initio* methods even in the near future.

For tetrahedral semiconductors, chemical intuition leads one to consider a minimal sp^3 basis on various kinds of atoms in the solid, and interactions only between the nearest-neighbor atoms seem necessary. Such a model describes the valence-band electronic structure with a limited accuracy, however, it is now well established that such a minimal model cannot reproduce the band gap,[2,3] performing even worse in describing the overall conduction-band electronic structure. In order to obtain an accurate estimate of the bandgap, Vogl and coworkers[4] added a fictitious s^* orbital to the sp^3 basis. Adjusting the various electronic parameters for the sp^3s^* TB model, it was possible to simulate the conduction- and valence-band extremal energies, thereby yielding the correct bandgap. However, this approach failed to account for the band dispersions even for the lowest unoccupied band. This failure is not surprising in view of the fact that the inclusion of the s^* orbital and the associated electronic parameter strengths are merely *ad hoc* parameters without any rigorous physical basis. However, almost all efforts in obtaining TB parametrization to describe the electronic structures of such semiconductors have proceeded along these lines; calculations for a number of tetrahedral semiconductors have resulted in the establishment of a *universal* sp^3s^* model based on Harrison's d^{-2} law for the interatomic matrix elements of the TB Hamiltonian.[4] The *universal* model is useful as only the interatomic distances are required to obtain the interaction parameters, but its applicability is limited as it does not give a good decription of the unocupied part, e.g., as discussed in the case of GaP.[4] Further improvements in the TB model were achieved by incorporating *d* orbitals in the basis.[5,6] Recently, a TB model based on the $sp^3d^5s^*$ basis set was employed for the group IV and III–V semiconductors.[7] This empirical model based on the nearest-neighbor interactions gives a good description of the electronic structure of these semiconductors, especially at high-symmetry points.

The need for a physical and accurate parametrization capable of describing both valence- and conduction-bands, and not merely the bandgap, of these semiconductors is evident. There are direct experimental probes such as the photoemission and inverse photoemission that map out the density of states (DOS) of the valence and conduction band regions. An analysis of such experiments requires a suitable TB parametrization that work equally well for the occupied as well as the unoccupied states. Furthermore, it is possible to obtain

experimental information on the partial density of states by using the site and angular momentum specific x-ray emission and absorption experiments; it is then desirable to have a TB model excluding the fictitious s^* orbital. Additionally, we have recently found[8] in the context of InP that even $sp^3d^5s^*$ TB parametrization does not work very well to describe the changes in the electronic structure as a consequence of spatial localization in nanometric clusters. Thus, it appears highly desirable to analyze the electronic structures of such semiconductors and thereby construct a physical as well as minimal model that would work satisfactorily for all these diverse cases.

In order to achieve this, we first study the linearized muffin-tin-orbital (LMTO) method[9,10] Derived DOS, partial density of states (PDOS), and the crystal orbital Hamiltonian population (COHP) to establish the relative importance of various orbitals in bonding as well as in determining the details of the electronic structure in different energy regions. This helps us to identify the important orbitals. From this analysis we construct the minimal model, without the s^* orbital. Since we construct the final TB model in successive steps of including various interactions, we understand in detail the influence of each of these improvements to modify the energy dispersions of various bands. Our final results for the II-VI semiconductors using the sp^3d^5-orbital basis are in excellent agreement with the LMTO calculations and the various interaction parameters obtained here obey the universal scaling law.

II. METHODOLOGY

The band structures of the $A^{\mathrm{II}}B^{\mathrm{VI}}$-type semiconductors, where $A=$ Zn, Cd, Hg and $B=$ S, Se, Te are calculated using the LMTO method in the atomic sphere approximation (ASA). The zinc-blende structure, which has one formula unit of $A^{\mathrm{II}}B^{\mathrm{VI}}$ per unit cell, has been studied. The basis set of *s*, *p*, and *d* orbitals was used for both the cation and the anion for all the compounds. Empty spheres were introduced in all cases in order to keep the overlap of atomic spheres within 16% in every case. Only *s* orbital is used for the empty spheres. The self-consistency was achieved with 28 *k*-points in the irreducible Brillouin zone and band dispersions and density of states were obtained in each case.

In order to obtain a detailed understanding of the origin of various features in the electronic structure, we also calculate the partial densities of states corresponding to cation and anion *s*, *p*, and *d* states. While the partial densities of states provide us with the information concerning the relative contributions of various orbitals at different energy regions, it cannot provide any *k*-dependent information. In order to obtain such momentum-related information, we have additionally analyzed the orbital character of the band-eigen states and shall present these in terms of the so-called ''fatband'' representation of the band dispersions. However, such analysis does not provide an insight on the range of interactions important for the system. The range of interaction is one of the most important ingredients to determine the suitable tight-binding model, as it dictates whether a nearest-neighbor-only model is sufficient or there is a need to include farther neighbor interactions. This issue can be addressed by computing the crystal orbital Hamiltonian population (COHP) for various pairs of orbitals and atoms, as it provides the relative contributions to bonding arising from different interactions in the system.[11]

The tight-binding calculations were performed using the Hamiltonian

$$\mathbf{H}=\sum_{il_1\sigma}\epsilon_{l_1}a^{\dagger}_{il_1\sigma}a_{il_1\sigma}+\sum_{ij}\sum_{l_1,l_2,\sigma}(t^{l_1l_2}_{ij}a^{\dagger}_{il_1\sigma}a_{jl_2\sigma}+\mathrm{H.c.}) \tag{1}$$

where, the electron with spin σ is able to hop from the orbitals labeled l_1 with onsite energies equal to ϵ_{l_1} in the ith unit cell to those labeled l_2 in the jth unit cell, with the summations over l_1 and l_2 running over all the orbitals considered on the atoms in a unit cell, and i and j over all the unit cells in the solid. Thus, any orbital in the solid can be defined with the two indices, i and l_1. The hopping interaction strength ($t^{l_1l_2}_{ij}$) depends on the nature of the orbitals involved as well as on the geometry of the lattice.[1] To start with, we estimate the values of the various onsite energies (ϵ's) and hopping interactions (t's) from the LMTO band dispersions and the density of states. Then, a least-squared-error fitting is carried out by varying the ϵ's and t's, calculating the band dispersions at a number of high-symmetry points and then comparing with the LMTO band dispersions. In the following section, we present the detailed analysis with the help of ZnS as an illustrative example; the results obtained from all other systems are very similar.

III. RESULTS AND DISCUSSION

In Fig. 1(a), we show the LMTO-derived band dispersions for ZnS along various symmetry directions. The lowest-lying band at about -12 eV is due to S *s* states, while the group of five flat bands near -6.4 eV arises from Zn *d* states. The main part of the valence-band region in ZnS appearing between -5.4 and 0 eV is contributed by three strongly dispersing bands arising primarily from the S-*p* states. The lowest-lying conduction band centered around 4 eV is nominally the Zn-*s* derived band, while the next three bands are attributed to Zn-*p* states. The parts of bands appearing at the top of the figure are contributed dominantly by higher-lying states, such as the S *d* levels. The band gap appearing at the Γ point is about 3.2 eV in this calculation. These results are consistent with the previously published band structure of ZnS.[12]

These results suggest that main parts of the valence and the conduction bands in ZnS across the band gap are essentially due to Zn *s*, *p* and S *s*, *p* states, suggesting a TB model consisting only of these levels as the simplest possible starting point.This point of view also makes chemical sense as the tetrahedral coordination around both Zn and S can be easily achieved in terms of the sp^3-hybrid orbitals. However, we show that such a simplistic model performs very poorly in describing the electronic structure. For this purpose, we carried out a detailed fitting of the six corresponding LMTO bands in terms of a nearest-neighbor TB model with the sp^3

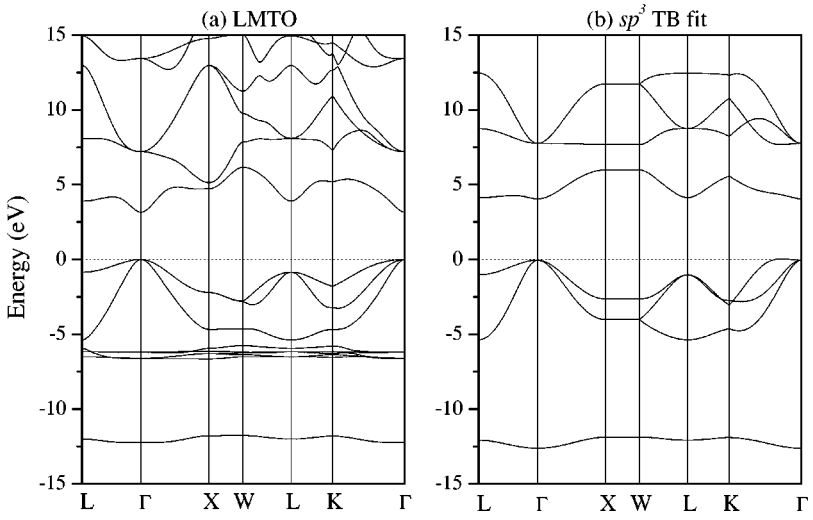

FIG. 1. Band dispersions for the zinc-blende ZnS (a) LMTO results using the *s*, *p* and *d* orbital basis on both Zn and S, (b) the tight-binding results for sp^3-orbital basis fit to the LMTO results. The zero of the energy scale is set at the top of the valence band.

basis. The resulting best description is shown in Fig. 1(b) in terms of the TB band dispersions with the optimized TB parameters. The Zn *d* bands near -6.4 eV and high-lying S *d* bands are naturally missing in the TB results. We find that the low-lying S *s* band is reasonably well described in this simplest model. However, the TB band dispersions for both the valence and the conduction bands are considerably different from those in the LMTO calculation. For example, the band dispersions along X-W-L-K-Γ within the valence-band region are drastically different between the two calculations. Moreover, not only the band gap is substantially wrong in the TB results, the curvature of the lowest lying conduction band near the Γ point is very poorly described within the TB model. The results clearly suggest the need to go beyond the simplest sp^3-nearest-neighbor TB model to provide a realistic description of the electronic structure of ZnS.

In order to understand the origin of these discrepancies, we plot the total as well as various partial DOS of ZnS in Fig. 2, with the Zn-related partial DOS in Fig. 2(a) and those related to the S site in Fig. 2(b). Focussing on the energy region for the discrepancies discussed above, we note that the valence-band features appearing between -5.4 and 0 eV are indeed dominated by S *p* states [Fig. 2(b)]; however, these states have substantial admixture from the Zn-*p* and *d* states [Fig. 2(a)]. Since the band formation in a nearest-neighbor model is entirely due to S-Zn interactions, it is obvious that Zn *d* states, contributing as much as the Zn-*p* states in the formation of the valence band, cannot be left out of any realistic description of the valence-band region of ZnS. Likewise, it is evident in the results for the conduction-band region in Fig. 2, particularly in the energy region approximately between 7 and 12 eV, that the S *d* contributions are almost dominant. This must arise from very large Zn *p*-S *d* interactions in forming the upper part of the conduction-band region, establishing the need to include the S *d* states also in the TB basis for a satisfactory description of the electronic structure comprising both valence- and conduction-band regions.

In order to obtain a more detailed understanding, as well as insight in the momentum-specific discrepancies, we present the LMTO band dispersions along the symmetry lines in the fatband representation in six different panels in Fig. 3. While the band dispersions in each of these six panels are identical, the width (or the ''fatness'') associated with each band at every *k* point is proportional to the orbital character represented in that panel; for example, Fig. 3(a) shows the contribution of Zn *s* states to each of the band eigenstates. These results clearly establish the detailed nature of the band states. For example, the band dispersion near -12 eV is dominated by S *s* states [Fig. 3(d)], formed via the interactions with Zn *s*, *p* and *d* states [see Fig. 3(a–c)]. Likewise, the flat bands near -6.4 eV are primarily Zn *d* bands [Fig. 3(c)] formed via the interactions with the S *p*

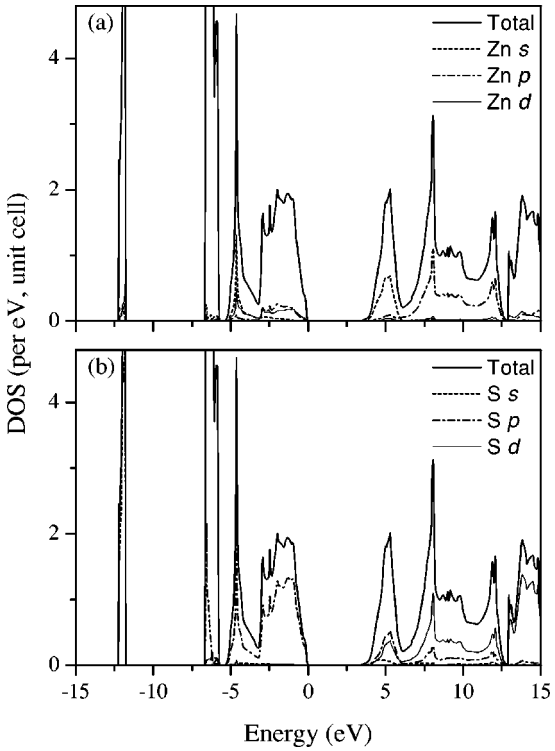

FIG. 2. Density of states and partial density of states for zinc-blende ZnS calculated using LMTO-ASA method: (a) Zn *s*, *p* and *d* PDOS; (b) S *s*, *p* and *d* PDOS

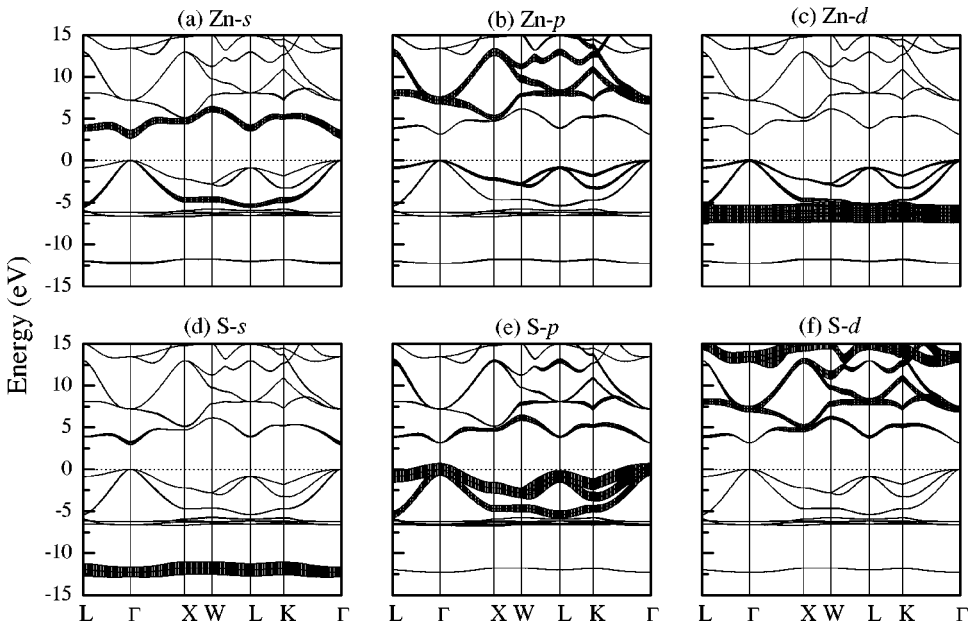

FIG. 3. Band dispersions for the zinc-blende ZnS showing fat-bands for (a)Zn *s*, (b) Zn *p*, (c) Zn *d*, (d)S *s*, (e) S *p* and (f) S *d*.

states [Fig. 3(e)]. More importantly, the three strongly dispersing bands in the valence-band region have the S *p* character [Fig. 3(e)], formed due to substantial S(p)-Zn (s, p, and d) interactions [Figs. 3(a–c)], confirming the essential role played by Zn *d* states in determining the valence-band electronic structure. Likewise, the extensive S *d* contributions in all the conduction-band states are also evident in Fig. 3(f). The inability of the sp^3 model to describe the curvature

TABLE I. Tight-binding parameters obtained from the least-square-error fit to LMTO band dispersions for the nine II-VI semiconductors in the sp^3d^5 basis with only the nearest-neighbor Zn-S interactions. The first row lists the interatomic spacings in angstrom, the next eight rows contain the onsite energies for all the orbitals, e.g., the row for $d_c(t_2)$ lists the entries for the the t_2 *d*-orbital onsite energies for the cation. The subscript *a* denotes the anion. The last 11 rows list the Slater Koster parameters.[13] The last column shows the average value of the Slater Koster parameters multiplied by the square of the cation-anion distance, d^2.

	ZnS	ZnSe	ZnTe	CdS	CdSe	CdTe	HgS	HgSe	HgTe	Average SKK^*d^2
d (Å)	2.34	2.45	2.64	2.52	2.62	2.81	2.53	2.63	2.80	
s_c	0.92	0.74	1.06	0.47	0.30	0.40	−2.03	−2.05	−1.75	
p_c	8.40	8.38	7.24	7.94	7.91	7.21	7.89	7.68	7.12	
$d_c(t_2)$	−5.82	−6.16	−6.92	−6.83	−7.31	−7.97	−5.99	−6.15	−6.91	
$d_c(e)$	−6.21	−6.47	−7.24	−7.44	−7.81	−8.42	−6.31	−6.53	−7.21	
s_a	−10.33	−11.24	−10.68	−10.58	−11.45	−10.38	−11.04	−11.57	−10.49	
p_a	2.41	1.93	2.29	1.43	0.93	1.13	0.69	0.66	0.03	
$d_a(t_2)$	15.54	16.48	13.23	14.43	15.26	12.83	14.84	15.68	12.83	
$d_a(e)$	13.60	14.48	12.23	13.15	14.10	11.63	12.87	13.54	11.66	
$ss\sigma$	−1.35	−1.01	−0.54	−1.02	−0.74	−0.47	−1.07	−0.93	−0.74	−5.73
$sp\sigma$	2.45	2.33	2.26	2.12	2.06	1.93	1.92	1.85	1.82	13.95
$pp\sigma$	4.76	4.37	4.01	4.18	3.70	3.54	3.93	3.75	3.08	26.18
$pp\pi$	−0.84	−0.83	−0.95	−0.64	−0.67	−0.69	−0.69	−0.71	−0.86	−5.17
$ps\sigma$	−2.25	−1.89	−0.52	−1.99	−1.66	−0.94	−1.81	−1.87	−1.25	−10.36
$ds\sigma$	−0.05	−0.04	−0.00	−0.00	−0.01	−0.26	−0.72	−0.54	−0.52	−1.67
$dp\sigma$	1.37	1.19	1.29	1.75	1.52	1.52	1.45	1.42	1.29	9.61
$dp\pi$	−0.45	−0.39	−0.34	−0.35	−0.32	−0.27	−0.59	−0.50	−0.31	−2.61
$sd\sigma$	−2.59	−2.71	−3.05	−1.14	−1.22	−2.11	−0.94	−1.40	−1.79	−12.65
$pd\sigma$	−2.78	−2.78	−3.36	−1.29	−1.09	−2.42	−1.37	−1.45	−1.73	−13.62
$pd\pi$	2.31	2.42	2.27	2.15	2.38	1.90	2.014	2.21	1.82	14.49

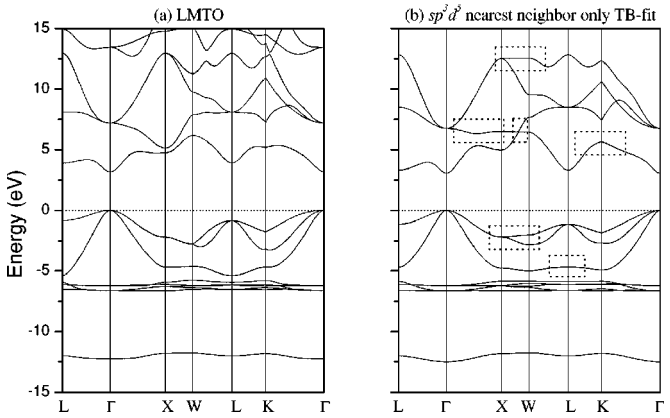

FIG. 4. Band dispersions for zinc-blende ZnS, (a) LMTO results and (b) tight-binding fitted results for the nearest-neighbor interactions only in the sp^3d^5-orbital basis on both Zn and S.

of the lowest conduction band near the Γ point (Fig. 1) can also be understood in terms of these fatbands. The band state at the Γ point is composed of Zn *s* admixed with S *s* states; however, these band states acquire rapidly changing contributions from S *p* and *d* states as *k* moves away from the Γ point, affecting the detail of the band dispersion in this region of the momentum space.

The above analysis clearly points to the need of including both Zn and S *d* states in the basis of the TB model for a realistic description of the valence- and conduction-band electronic structures of ZnS. While we have presented here the detailed analysis for only the case of ZnS, we carried out similar analysis for all the compounds and arrived at the same conclusion concerning the importance of cationic and anionic *d* states. Therefore, we carried out a detailed least-squared-error fitting of the LMTO derived band dispersions in terms of the TB dispersions with sp^3d^5 basis as a function of all the electronic parameters (on-site and hopping energies) appearing in the TB Hamiltonian. The fitting was carried out in two successive steps. First, we performed a fitting of all the 18 bands arising primarily from Zn and S *s*, *p*, and *d* states, though the S *d* derived bands appearing at a very high energy above the Fermi energy do not have any significant bearing on electronic, optical or chemical properties of the system. However, the inclusion of the S *d* derived band dispersions in the first step of fitting ensures that we use a realistic and physically sound value for the S *d* site energy. We then fix the S *d* site energy to this value in the second step of the fitting and reoptimize the other electronic parameters to arrive at the best description for the thirteen lowest bands with primarily Zn *s*, *p*, *d* and S *s*, *p* characters. The results of this optimization process are tabulated in Table I for all the compounds studied here, while the best-fit TB dispersions within this sp^3d^5 nearest-neighbor model for ZnS are compared with the *ab initio* LMTO dispersions in Fig. 4. The improvement in using the sp^3d^5 model compared to the results obtained from sp^3 model (Fig. 1) is evident in Fig. 4. We find that all the band dispersions, covering both the valence and conduction bands, as well as the curvature of the lowest conduction band near the Γ point are almost satisfactorily described. We believe that these parametrizations, , summarized in Table I, should already be useful in modeling these semiconductors to a large extent. However, we can still notice certain discrepancies between the LMTO and TB dispersions given in Fig. 4. The major deviations of the TB band dispersions from the LMTO ones are marked by rectangular boxes in Fig. 4.

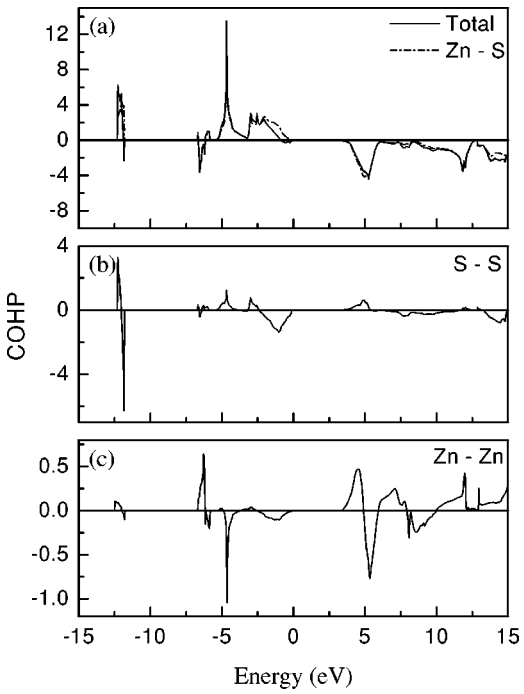

FIG. 5. COHP for zinc-blende ZnS. Top panel shows the total COHP alongwith the Zn-S interaction COHP. Middle panel shows the COHP for S-S interaction and the bottom panel contains the COHP for Zn-Zn interaction.

In order to understand the origin of these discrepancies, we show crystal orbital Hamiltonian population (COHP) analysis for ZnS in Fig. 5. The total COHP is compared with contributions arising from Zn-S interactions in Fig. 5(a). This clearly shows that the total COHP deviates significantly from that arising from Zn-S nearest-neighbor interactions alone, suggesting a longer-range interaction also playing a significant role in bonding. We show the COHP contributions arising from S-S and Zn-Zn interactions in Figs. 5(b) and 5(c), respectively. These results clearly show that while Zn-Zn interaction [Fig. 5(c)] is small and can possibly be neglected, S-S interaction [Fig. 5(b)] contributes significantly and is often comparable to Zn-S interactions in certain energy ranges. Thus, it is evident that a more accurate description of the electronic structure of ZnS must include next-nearest-neighbor S-S interactions along with the nearest-neighbor Zn-S interactions. Thus, we carried out a detailed fitting of the LMTO band dispersions in terms of a TB model in the sp^3d^5 basis, as before, but including the next-nearest-neighbor S-S interactions along with the nearest-neighbor Zn-S interactions. We follow the same two-step approach to the fitting, as described before. The resulting TB parameters for the best-fit results for each compound are given in Table II and an illustrative example of the simulated band dispersions are shown in Fig. 6 using the case of ZnS. Most of the

TABLE II. Tight-binding parameters obtained from the least-square-error fit to LMTO band dispersions for the nine II-VI semiconductors in the sp^3d^5 basis with the Zn-S and S-S interactions. The first row lists the interatomic spacings in angstrom, the next eight rows contain the onsite energies for all the orbitals, e.g., the row for $d_c(t_2)$ lists the entries for the the t_2 d-orbital onsite energies for the cation. The subscript a denotes the anion. The last fifteen rows list the Slater Koster parameters.[13] The last column shows the average value of the Slater Koster parameters multiplied by the square of the cation-anion distance, d^2.

	ZnS	ZnSe	ZnTe	CdS	CdSe	CdTe	HgS	HgSe	HgTe	Average SKK^*d^2
d (Å)	2.34	2.45	2.64	2.52	2.62	2.81	2.53	2.63	2.80	
s_c	2.29	1.40	0.50	1.44	0.83	0.50	−0.85	−0.95	−1.45	
p_c	9.32	9.21	8.36	8.22	7.80	7.78	8.16	8.35	7.76	
$d_c(t_2)$	−6.24	−6.46	−7.26	−7.53	−7.85	−8.46	−6.10	−6.66	−7.27	
$d_c(e)$	−6.16	−6.40	−7.21	−7.38	−7.74	−8.39	−6.81	−6.46	−7.18	
s_a	−10.66	−11.21	−9.82	−10.58	−11.19	−9.70	−11.47	−11.93	−10.45	
p_a	3.17	2.06	1.12	3.42	2.43	1.06	2.59	1.45	0.72	
$d_a(t_2)$	15.31	16.10	13.08	14.32	15.12	13.20	14.72	15.42	12.76	
$d_a(e)$	13.63	14.53	12.29	13.16	14.11	11.62	12.92	13.58	11.66	
$ss\sigma$	−0.73	−0.74	−0.40	−0.72	−0.50	−0.00	−1.01	−0.88	−0.63	−4.08
$sp\sigma$	2.57	2.68	2.19	2.12	2.04	2.01	2.05	2.06	1.81	14.49
$pp\sigma$	4.95	4.63	3.99	4.40	4.06	3.83	4.16	4.03	3.63	28.01
$pp\pi$	−0.88	−0.78	−1.05	−0.44	−0.49	−0.77	−0.48	−0.50	−0.64	−4.51
$ps\sigma$	−2.11	−1.28	−1.37	−1.41	−1.70	−0.86	−1.00	−0.90	−1.14	−8.66
$ds\sigma$	−0.67	−1.33	−0.32	−0.73	−0.69	−0.35	−1.17	−1.27	−0.74	−5.36
$dp\sigma$	0.91	0.84	1.04	0.80	0.67	1.47	0.51	0.93	0.70	5.98
$dp\pi$	−0.43	−0.20	−0.10	−0.55	−0.51	−0.17	−0.38	−0.43	−0.37	−2.32
$ss\sigma(2)$	−0.10	−0.09	−0.06	−0.04	−0.06	−0.01	−0.00	−0.02	−0.03	−0.30
$sp\sigma(2)$	0.32	0.42	0.00	0.01	0.00	0.30	0.21	0.23	0.26	1.30
$pp\sigma(2)$	0.61	0.58	0.50	0.48	0.46	0.37	0.52	0.47	0.38	3.23
$pp\pi(2)$	−0.06	−0.02	−0.01	−0.03	−0.02	−0.01	−0.03	−0.02	−0.02	−0.16
$sd\sigma$	−2.61	−2.87	−2.69	−1.29	−1.44	−1.90	−0.95	−1.47	−1.85	−12.70
$pd\sigma$	−3.85	−4.19	−3.98	−2.61	−2.64	−3.46	−2.73	−3.06	−3.06	−22.10
$pd\pi$	2.80	2.81	2.55	2.34	2.49	2.24	2.17	2.31	2.07	16.20

deviations in the band dispersions observed in the case of the nearest-neighbor model (Fig. 4) are largely removed, except for the band crossing along the X-W direction for the conduction bands in the TB result, shown in Fig. 6, leading to an excellent agreement with the *ab initio* results. We have further verified the reliability of these parameters in describing, not only the band dispersions along the symmetry directions, but also the overall electronic structures by computing the density of states within the TB model. In Fig. 7, we show the comparison of DOS obtained from LMTO and that from the

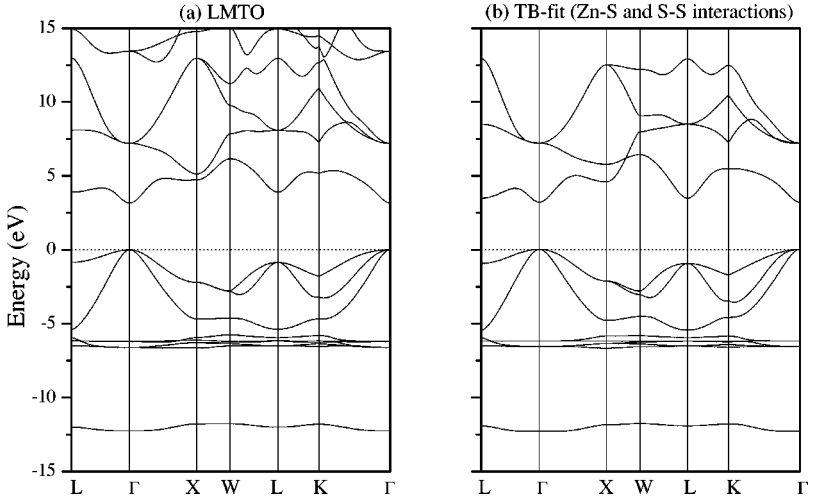

FIG. 6. Comparison of band dispersions for ZnS from (a) LMTO and (b) tight-binding fit with the sp^3d^5 orbital basis on both Zn and S. Both Zn-S and S-S interactions are included in the TB model.

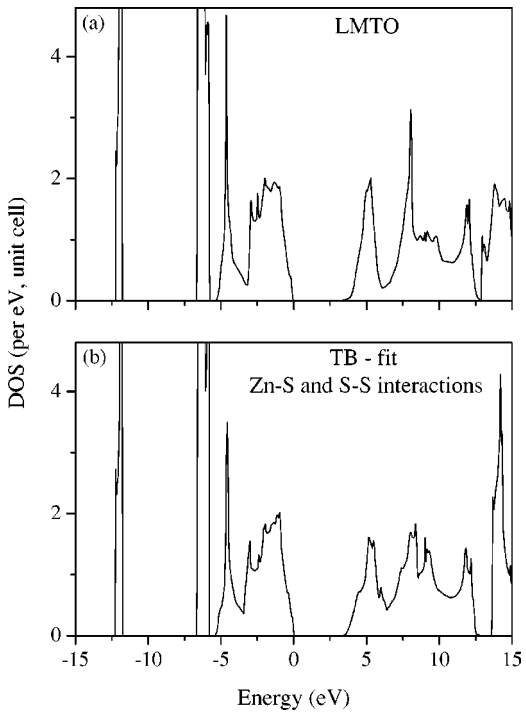

FIG. 7. Comparison of total density of states for ZnS from (a) LMTO and (b)tight-binding fit with the sp^3d^5-orbital basis on both Zn and S. Both Zn-S and S-S interactions are included in the TB model.

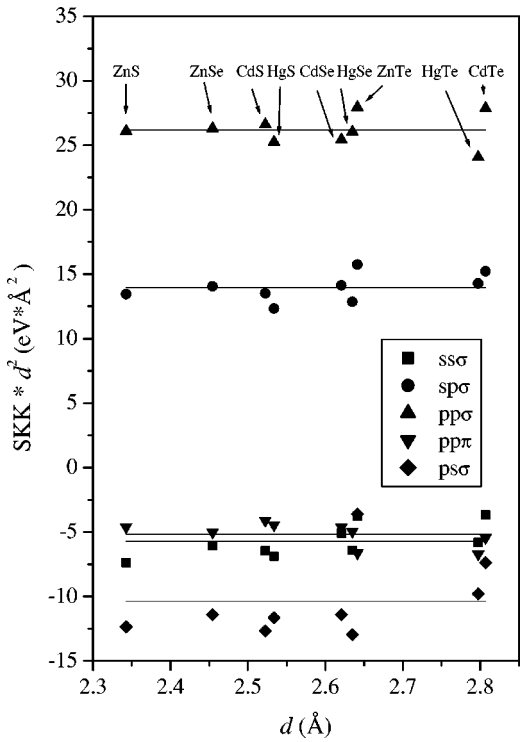

FIG. 8. SKK*d^2 versus d for all the II-VI semiconductors studied using the TB model with the sp^3d^5 basis on both the anion and the cation with only nearest-neighbor interactions; SKK represents the various hopping parameters and d is the distance between the cation and the anion. The plot establishes the scaling behavior of the hopping parameters $ss\sigma$, $sp\sigma$, $pp\sigma$, $pp\pi$, and $ps\sigma$.

present TB model for the case of ZnS over the valence- and conduction-band regions. The figure shows a very good agreement between the two.

An important step in demonstrating the usefulness of such parametrized tight-binding approaches was realized by the bond orbital model proposed by Harrison[3] who showed that the hopping interaction strengths follow a universal scaling law with the distance between the two orbital sites. For a large number of systems, it was shown that the Slater-Koster parameters have a dependence of d^{-2}, where d is the distance between the two sites connected by the hopping integral. This observation ensures that the extracted parameters are transferable to other crystal structures. This approach was further extended[4] to include a description of the lowest conduction band along with the valence band within a nearest-neighbor sp^3s^* model.

In order to establish the transferability, and consequently the usefulness, of the hopping parameter values obtained here, we have examined the scaling behavior of these parameters. In Fig. 8, we plot the various hopping interaction strengths (SKK) obtained within the nearest-neighbor-only model (Table I) multiplied by d^2 as a function of d for all the compounds. This figure clearly shows that the parameter values follow the d^{-2} scaling law reasonably well, with SKK*d^2 being nearly independent of d for each type of hopping parameters, as shown in the figure by the horizontal lines representing the average SKK*d^2 values which are also listed in Table I. We find that the primary deviations from the scaling laws are for the three compounds with Te, namely, ZnTe, HgTe, and CdTe, while the compounds of S and Se obey the scaling law considerably better. It turns out that even for the tellurides, the deviations from the scaling law do not significantly vitiate the description of the electronic structure. To illustrate this point, we show in Fig. 9 the band dispersions obtained for ZnTe, which exhibits one of the largest deviations from the expected scaling law. Figure 9(a) describes the *ab initio* band dispersions obtained within LMTO, while Fig. 9(b) shows the best fit obtained with tight-binding nearest-neighbor-only model. The corresponding parameter values are given in Table I and the data points are plotted in Fig. 8 multiplied by the corresponding d^2. The band dispersions obtained within the same model, but with parameter values corresponding to the average (SKK*d^2) instead of the best-fit optimized parameters, are shown in Fig. 9(c). A comparison of Fig. 9(b) and 9(c) shows hardly any difference between the two, both providing excellent description of the *ab initio* band dispersions shown in Fig. 9(a). This indicates that the parameters obtained within the nearest-neighbor-only model are transferable to other cases.

We have also examined the scaling behavior of the hopping parameters obtained with the next nearest-neighbor model (Table II) and found a similar d^{-2} dependence. The corresponding average values of SKK*d^2 are also given in Table II. Using these average values of the hopping parameters we have calculated the band dispersions for ZnTe, shown in Fig. 9(d). These band dispersions also provide an excellent description of the band dispersions obtained within the *ab initio* approach, shown in Fig. 9(a).

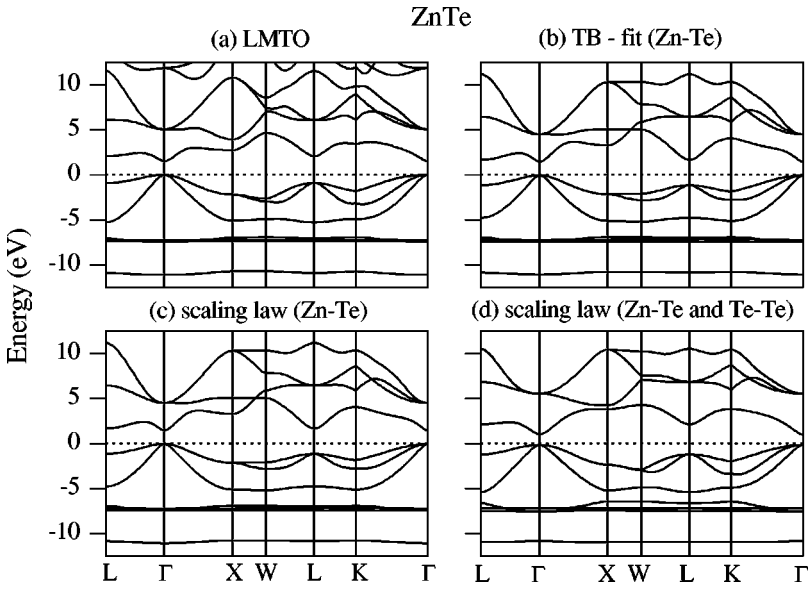

FIG. 9. Comparison of band dispersions for ZnTe obtained from (a) LMTO, (b) TB-fit using the sp^3d^5-orbital basis with nearest-neighbor-only interactions, (c) Scaling parameters obtained from the above model. The parameters are extracted from the SKK* d^2 values in Table I. (d) scaling parameters obtained from the TB-fit model with the anion-anion next nearest-neighbor interactions (values from Table II).

IV. CONCLUSION

In conclusion, we have presented a systematic development of parametrized tight-binding model for the description of the electronic structures of group II-VI semiconductors comprising both the valence and the conduction bands. We analyze the nature and origin of bonding as well as the atomic orbital contributions to each band eigen-states to arrive at the necessary minimal model involving sp^3d^5 orbitals at the cationic and the anionic sites, obviating the need to use any fictitious s^* orbital in the basis. Even a nearest-neighbor-only model is found to provide a fair description of the *ab initio* band dispersions and the density of states over a wide energy range covering the entire valence- and conduction-band regions. The obtained hopping parameters are shown to observe the d^{-2} scaling law of the bond orbital model proposed by Harrison. Furthermore, we also obtain the parameter values in a next nearest-neighbor tight-binding model that further improves the agreement of this empirical approach to the *ab initio* results, capturing some subtle features in bonding in these compounds, particularly involving the top of the valence band.

ACKNOWLEDGMENTS

We thank O.K. Anderson and O. Jepsen for providing the LMTO code and P. Mahadevan and T. Saha-Dasguta for useful discussions.

*Also at Jawaharlal Nehru Center for Advanced Scientific Research; Electronic mail address: sarma@sscu.iisc.ernet.in

[1] J. C. Slater and G. F. Koster, Phys. Rev. B **94**, 1498 (1954).
[2] D. J. Chadi and M. L. Cohen, Phys. Status Solidi B **68**, 405 (1975).
[3] W. A. Harrison, *Electronic Structure and Properties of Solids* (Freeman, San Francisco, 1980).
[4] P. Vogl, H. P. Hjalmarson, and J. D. Dow, J. Phys. Chem. Solids **44**, 365 (1983).
[5] S. L. Richardson, M. L. Cohen, S. G. Louie, and J. R. Chelikowsky, Phys. Rev. B **33**, 1177 (1986).
[6] Y. C. Chang and D. E. Aspnes, Phys. Rev. B **41**, 12 002 (1990).
[7] J.-M. Jancu, R. Scholz, F. Beltram, and F. Bassani, Phys. Rev. B **57**, 6493 (1998).
[8] Sameer Sapra, Ranjani Viswanatha, and D. D. Sarma (unpublished).
[9] O. K. Andersen, Phys. Rev. B **12**, 3060 (1975).
[10] O. K. Andersen and O. Jepsen, Phys. Rev. Lett. **53**, 2571 (1984).
[11] R. Dronskowski and P. E. Blochl, J. Phys. Chem. **97**, 8617 (1993).
[12] M. L. Cohen and J. R. Chelikowsky, *Electronic Structure and Optical Properties of Semiconductors*, (Springer-Verlag, Berlin, 1989).
[13] The convention we have used for the Slater Koster parameters indicates the first orbital is on the cation and the second orbital on the anion. Second nearest-neighbor interactions between anion-anion are marked by a 2 in the brackets.